Proceedings of the Combustion Institute

The effect of pressure on the hydrodynamic stability limit of premixed flames

--Manuscript Draft--

Manuscript Number:	PROCI-D-19-00409R3
Article Type:	4. Laminar Flames
Keywords:	Darrieus-Landau instability; Direct numerical simulation; Cut-off scale; pressure effects
Corresponding Author:	Antonio Attili RWTH Aachen University Aachen, GERMANY
First Author:	Antonio Attili
Order of Authors:	Antonio Attili
	Rachele Lamioni
	Lukas Berger
	Konstantin Kleinheinz
	Pasquale E. Lapenna
	Heinz Pitsch
	Francesco Creta
Abstract:	The effect of pressure on the hydrodynamic stability of lean methane-air premixed flames is investigated with Direct Numerical Simulation based on multi-step chemistry and using a simplified one-step chemistry formulation. The dependency on pressure p of the cut-off length scale λ_c, that separates stable from unstable wavelengths of the initial perturbation, is computed for a number of different conditions. An increase of pressure causes a significant decrease of the cut-off length, as observed already in previous simulations and experiments. However, this decrease cannot be ascribed only to the decreased flame thickness due to elevated pressures, but the cut-off is reduced significantly even if normalized by either the thermal flame thickness l_T or the diffusive flame thickness l_D. For the conditions analyzed, the cut-off can be well approximated by the power-law $\lambda_c \propto p^{-0.8}$, while the thermal and diffusive flame thicknesses, in accordance with previous experiments, are proportional and scale as $l_T \propto l_D \propto p^{-0.3}$. Therefore, the non-dimensional cut-off scales as $\lambda_c/l_T \propto \lambda_c/l_T \propto p^{-0.5}$. This behavior is linked to the increase of the Zeldovich number with pressure, caused by higher inner layer temperatures at higher pressures, which is a result of increased importance of chain termination reactions. The same behavior is observed also in a one-step chemistry approach if the Zeldovich number, appearing explicitly in the one-step

	model equations, is varied with pressure according to the results from multi-step chemistry. The analysis is extended to the non-linear phase of the instability, when typical strong cusps are observed on the flame surface, simulating a two-dimensional slot burner for different pressures; it is confirmed that the same pressure effects are observed also in more complex settings and in the non-linear regime.

The effect of pressure on the hydrodynamic stability limit of premixed flames

Antonio Attili[a,*], Rachele Lamioni[b], Lukas Berger[a], Konstantin Kleinheinz[a], Pasquale E. Lapenna[b,c], Heinz Pitsch[a], Francesco Creta[b]

[a] *Institute for Combustion Technology, RWTH Aachen University, 52062 Aachen, Germany*
[b] *DIMA, Sapienza University of Rome, 00189 Rome, Italy*
[c] *ENEA C.R. Casaccia, 00123 Rome, Italy*

Abstract

The effect of pressure on the hydrodynamic stability limits of lean methane-air premixed flames is investigated with Direct Numerical Simulation based on multi-step chemistry and using a simplified one-step chemistry formulation. The dependency on pressure p of the cut-off length scale λ_c, that separates stable from unstable wavelengths of the initial perturbation, is computed for a number of different conditions. An increase of pressure causes a significant decrease of the cut-off length, as observed already in previous simulations and experiments. However, this decrease cannot be ascribed only to the decreased flame thickness due to elevated pressures, but the cut-off is reduced significantly even if normalized by either the thermal flame thickness ℓ_T or the diffusive flame thickness ℓ_D. For the conditions analyzed, the cut-off can be well approximated by the power-law $\lambda_c \propto p^{-0.8}$, while the thermal and diffusive flame thicknesses, in accordance with previous experiments, are

*Corresponding author
Email address: a.attili@itv.rwth-aachen.de (Antonio Attili)

proportional and scale as $\ell_T \propto \ell_D \propto p^{-0.3}$. Therefore, the non-dimensional cut-off scales as $\lambda_c/\ell_T \propto \lambda_c/\ell_D \propto p^{-0.5}$. This behavior is linked to the increase of the Zeldovich number with pressure, caused by higher inner layer temperatures at higher pressures, which is a result of increased importance of chain termination reactions. The same behavior is observed also in a one-step chemistry approach if the Zeldovich number, appearing explicitly in the one-step model equations, is varied with pressure according to the results from multi-step chemistry. The analysis is extended to the non-linear phase of the instability, when typical strong cusps are observed on the flame surface, simulating a two-dimensional slot burner for different pressures; it is confirmed that the same pressure effects are observed also in more complex settings and in the non-linear regime.

Keywords:
Darrieus-Landau instability, Direct Numerical Simulation, Cut-off scale, Pressure effects

---

1. Introduction

Premixed flames subject to perturbations are prone to different intrinsic instabilities [1], caused by thermal expansion and, potentially, differential transport of mass and heat. In the hydrodynamic, or Darrieus-Landau (DL), instability [2, 3], short perturbation wavelengths are stabilized by diffusive effects, while long wavelengths are amplified and eventually stabilized into characteristic cusp-like structures by the non-linear underlying Huygens propagation mechanism. For given conditions, a cut-off wavelength that separates stable from unstable perturbations exists and defines an additional

intrinsic flame length scale in addition to the usual flame thickness and other scales. The dependence of the cut-off scale on different flame conditions, such as equivalence ratio, temperature, and pressure, is an important information to assess the likelihood of instability development. The stability limits and instability patterns have been extensively investigated experimentally [4–10] and with a number of analytical and numerical approaches with rather different geometrical and modeling complexity [1, 11–24]. Pressure is recognized as an important parameter due to its strong effects on the thickness and the speed of premixed flames. It is well known that an increase of pressure causes a significant increase of the propensity of the flame to become unstable and to show the characteristic Darrieus-Landau cusps [4, 5, 8, 10, 25]. However, the mechanism responsible for the pressure effects and a conclusive assessment whether the increased instability propensity is just a consequence of the decreased flame thickness deserve further investigation. In this work, the onset of the Darrieus-Landau instability is investigated in a series of methane-air flames at different pressures, by means of Direct Numerical Simulation (DNS), employing both a detailed multi-step chemistry model and a simplified one-step formulation.

2. Physical models, numerical methods, configurations, and methodologies to assess the flame stability limits

The analysis of the cut-off length scale is performed using two different approaches in order to disentangle the effects of the different phenomena that characterize flames at increasing pressure: *(i)* Direct Numerical Simulation (DNS) employing finite rate chemistry and a multi-step mechanism

to describe chemical reactions and *(ii)* single-step chemistry DNS based on temperature and a deficient reactant. The two models constitute standard practice in the simulation of combustion and their detailed description is available in classical references [26]. In all cases, the reactive, unsteady Navier-Stokes equations are solved in the low Mach number limit and the mixture obeys the ideal gas equation of state.

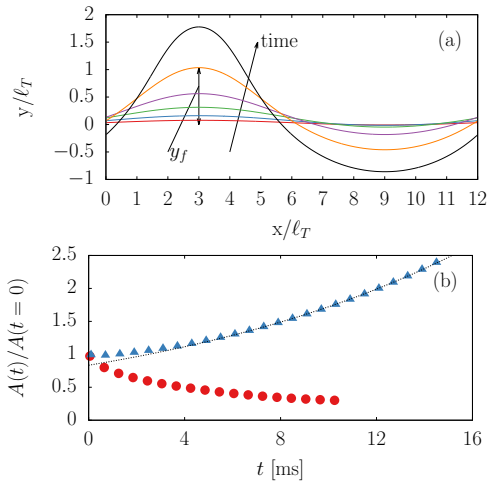

Figure 1: (a) Temporal evolution of the isocontour of temperature corresponding to the peak reaction rate for an unstable flame at unburned temperature $T_u = 300$ K, equivalence ratio $\phi = 0.7$, and pressure $p = 8$ atm, initially perturbed with a wavelength λ equal to 12 thermal flame thickness. The axis are scaled with the thermal flame thickness ℓ_T. (b) Time evolution of the amplitude for a stable ($T_u = 300$ K, $\phi = 0.7$, and $p = 1$ atm, red) and an unstable flame ($T_u = 300$ K, $\phi = 0.7$, and $p = 8$ atm, blue), both initially perturbed with a wavelength $\lambda = 12\ell_T$. All the results are obtained with the multi-step chemistry.

In the multi-step DNS approach, the equation for the full set of chemical species and temperature [27–29] are solved employing a finite-rate multi-step model with 16 species and 72 reactions [28, 30]. The transport properties

are evaluated using a mixture averaged model for the temperature equation [31] while the species diffusivities are computed prescribing spatially homogeneous values of the species Lewis numbers Le_i. In most of the cases, all the Lewis numbers are set to one, while selected cases have been also simulated with non-unity Lewis numbers. In cases with non-unity Lewis numbers, those are evaluated at the thermodynamic conditions of the fully burned mixture. The equations are solved with a semi-implicit finite difference code [32]. Spatial derivatives are discretized with second order finite differences for the momentum equation and the scalar diffusive terms, while a third order WENO scheme [33] is used for the convective term in the scalar equations. The Strang operator splitting is applied to the chemical source term, which is integrated with the stiff ODE solver CVODE [34].

In order to determine the dependence of the stability limit on pressure, it is necessary to compute the growth rate of an initial perturbation, superimposed on an otherwise planar flame, for different wavelengths λ of the perturbation, and identify the wavelength across which a transition from a negative to positive growth rate is observed. The function $\omega(k)$ relating the growth rate ω to the initial perturbation wave-number $k = 2\pi/\lambda$ is the dispersion relation, while the value of the wavelength corresponding to the transition from negative to positive growth rates identifies the cut-off scale λ_c. For this purpose, a fully-developed planar laminar flame is initialized in a two dimensional domain sufficiently large to allow an unconfined evolution of the flame. The flow is periodic in the spanwise direction x, while inflow and outflow boundary conditions are specified at the two boundaries in the streamwise direction y. The domain is discretized ensuring 40 to 50

points in the thermal flame thickness $\ell_T = (T_b - T_u)/(\partial T/\partial y)_{max}$, where T_b and T_u are the burnt and unburnt temperature, and $(\partial T/\partial y)_{max}$ the maximum temperature gradient in a one-dimensional planar laminar flame. This choice for the numerical resolution is appropriate, since it has been verified that using half of the points in every direction produced the same results. In order to evaluate the cut-off scale λ_c efficiently, the size of the domain in the spanwise direction is set equal to the perturbation length λ. Temperature and species mass fractions, computed with the FlameMaster code [35] in a one-dimensional laminar flame, are mapped in the two-dimensional domain to initialize the simulation. In order to create a wavy initial pattern at time $t = t_0$, the one-dimensional profiles are slightly shifted in the streamwise direction y by a different distance $y_f(x, t_0)$ for each spanwise location x using a sinusoidal function with wavelength λ. The amplitude of the initial perturbation has been set to $0.04\ell_T$, which is a small value that guarantees the existence of an initially linear regime that can be used to extract meaningful values of the growth rate. The amplitude $A(t)$ of the function $y_f(x, t)$ is monitored in time and the observation of an increase or decrease of $A(t)$ allows to infer the stability of the flame for the given wave-number. The amplitude is computed as the maximum value of the sinusoidal that best fits the function $y_f(x, t)$ in a least-squares sense. It is worth noting here that the sinusoidal fitting is very accurate for a rather long time during the initial linear phase of the instability and different approaches tested for the evaluation of the growth rate produced negligibly different results, pointing out the robustness of the methodology employed.

A typical evolution of the function $y_f(x, t)$ for an unstable flame is shown

in Fig. 1. The initial perturbation grows in time preserving a sinusoidal shape for a certain time. For large times, the non-linear behavior manifests itself in a significant asymmetry of the isoline and in the onset of characteristic cusp-like structures. Figure 1 shows also the time evolution of the amplitude $A(t)$ of the function $y_f(x,t)$ for a stable and an unstable flame. An exponential fit of the form ae^{bt} for the unstable case is also shown in Fig. 1. The instantaneous growth rate at the given wave-number $k = 2\pi/\lambda$ is computed from the amplitude as the semi-logarithmic derivative $\omega^*(k,t) = d[ln(A(t)/A(t=0))]/dt$; a time interval with a constant value of ω^* is identified and this constant value is then chosen to construct the dispersion relation $\omega(k)$.

As mentioned above, single-step chemistry has also been employed. The model is based on the following equations for temperature T_1 and a deficient reactant with mass fraction Y_1 [18]:

$$\rho\frac{\partial T_1}{\partial t} + \rho u \cdot \nabla T_1 = \nabla \cdot (\delta \nabla T_1) + \frac{\Omega}{\delta} \tag{1}$$

$$\rho\frac{\partial Y_1}{\partial t} + \rho u \cdot \nabla Y_1 = \nabla \cdot (\frac{\delta}{Le}\nabla Y_1) - \frac{\Omega}{\delta} \tag{2}$$

where δ is a dimensionless flame thickness, u is the gas velocity, Le the Lewis number. The source/sink term Ω is expressed, according to a one-step irreversible Arrhenius reaction, $\Omega = [Ze^2 Y_1/2Le] \exp[(Ze(1-T_1))/(1-(1-1/\sigma)(1-T_1))]$, where the expansion ratio σ is defined as the ratio of the densities of the unburned and the burned gas. The Zeldovich number is defined as $Ze = [E_a(T_b - T_u)]/[RT_b^2]$, where E_a is the activation energy of the single-step reaction of Arrhenius type while T_b and T_u are the burnt and unburnt temperatures [36, 37]. In order to have a comparison between the multi-step

DNS and the single-step model, the parameters that appear in the single-step model equations, i.e., the Zeldovich number Ze, the expansion ratio σ, and the Lewis number Le, are evaluated from a one-dimensional freely propagating flame computed with the multi-step chemistry model. As it will be verified in the following analysis, pressure has a negligible effect on the expansion ratio σ; therefore, the Zeldovich number is the main parameter that takes into account the pressure variation in the one-step chemistry formulation. In the single-step chemistry, it can be shown that the Zeldovich number can also be expressed as $Ze = 4(T_b - T_u)/(T_b - T_0)$, where T_0 is the cross-over (inner layer) temperature [36, 37]. This expression is used to specify the Zeldovich number in the one-step formulation, with T_0 being the temperature of maximum heat release in a one-dimensional flame with the multi-step chemistry [37]. Anyway, we observed that a definition of T_0 based on the maximum temperature gradient does not change the results. In order to perform the analysis efficiently, the non-dimensional thickness is defined as $\delta = l_D/\lambda$, where $l_D = D_{th}/S_L$ is the diffusive flame thickness and λ is the wavelength of the perturbation. The critical wavelength λ_c in the one-step chemistry approach is determined by identifying the critical δ_c of neutral growth of the perturbation. The configuration employed in the one-step chemistry cases is the same of that used for the multi-step approach. Numerical simulations with one-step chemistry are carried out using a well-established numerical framework for the investigation of DL instability [18, 22, 23]. The governing equations in the one-step approach are solved using an equation-of-state independent version [38–40] of *nek5000*, which is a massively parallel flow solver based on the spectral element method [41].

The results for the linear regime in the configuration described above are reported in Sec 3.1 for both chemistry models.

Table 1: Parameters for the DNS with the Bunsen configuration.

Case name	SP-1	UP-8
p (atm)	1	8
ℓ_T (mm)	0.572	0.284
λ_c	$14\ell_T$	$6\ell_T$
H	6.8mm ($12\ell_T$)	3.4mm ($12\ell_T$)
Domain size, $L_x \times L_y$	3Hx6H	3Hx5H
Grid size, $N_x \times N_y$	360×720	360×600
Resolution $\Delta x/\ell_T$, $\Delta y/\ell_T$	0.1	0.1
$U_b = 10S_L$ (m/s)	1.863	0.409
u'/S_L	0.79	0.79

Finally, a second configuration has been considered in order to verify that the results pertaining to the linear-regime of the intrinsic flame instability, can also be extended to the non-linear regime. A two-dimensional, planar slot flame is employed and the morphology of the flame surface for different values of pressure and characteristic length scale is investigated. For this configuration, a typical laminar triangular flame is perturbed with small broad-band velocity fluctuations with root mean square u' approximately 10% of the mean velocity U_b prescribed at the fresh mixture inlet. A coflow of fully burned product is imposed outside of the main jet with a velocity appropriately chosen to minimize the shear between the main jet and the coflow. Free-slip boundary conditions are prescribed on the lateral boundaries in the crosswise direction x, while an outflow is set at the end of the

domain in the streamwise direction y. A summary of the physical and numerical parameters for these DNS is presented in Tab. 1. The analysis focuses on two different cases, with identical thermo-chemical properties but different pressure. In this case, the solutions are obtained using the multi-step approach with unity Lewis numbers and the corresponding code and numerical methods described above. The results are reported in Sec 3.2.

3. Results

3.1. Linear regime: cut-off length scale

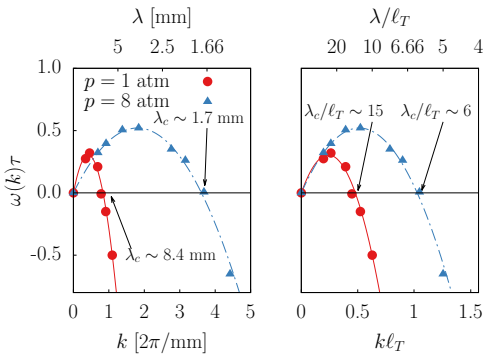

Figure 2: Growth rate of the perturbation $\omega(k)$ for different wavelengths $\lambda = 2\pi/k$ (dispersion relation) for two flames at different pressures, an equivalence ratio $\phi = 0.7$ and unity Lewis numbers, obtained with multi-step chemistry DNS: $p = 1$ atm (red circles) and $p = 8$ atm (blue triangles). The lines are fits to the DNS data. The results are shown in dimensional form (left panel) and non-dimensionalized with the thermal flame thickness and flame time (right panel).

The methodology described in Sec 2 has been applied to a number of different cases to compute the cut-off length scale and specifically to assess its dependence on pressure. Figure 2 shows the dispersion relation for two

cases characterized by identical thermochemical condition of the unburned mixture but two different pressures of 1 and 8 atm, respectively. The results are shown in both dimensional and non-dimensional units. In dimensional units, the comparison of the two dispersion relations reveals a significant decrease of the cut-off length scale λ_c from 8.4 to 1.7 mm when the pressure is increased from 1 to 8 atm. This behavior is not unexpected and has been observed in other situations [4, 10, 25] and somehow ascribed to the decreased flame thickness due to the elevated pressure. However, when the dispersion relations are normalized with the thermal flame thickness ℓ_T, the non-dimensional cut-off scale λ_c/ℓ_T still shows a significant dependence on pressure, proving that the scaling of the cut-off scale with the laminar flame thickness does not hold. The dependence of the cut-off length scale λ_c on pressure is summarized in Fig. 3(a). The figure also shows the thickness of the flame as function of the pressure. Since the internal flame structure in a multi-step chemical model might not be self-similar for different pressures, three different definitions of the laminar flame thickness are reported in the figure to check if different measures of the flame thickness could collapse the cut-off scale. The three definitions are: *(i)* the thermal thickness ℓ_T, *(ii)* the diffusive thickness $l_D = D_{th}/S_L$, and *(iii)* an inner layer thickness defined as the distance between the two points where the reaction rate of the progress variable is 20% of the peak. Comparing the variation with pressure of the cut-off length scale and the various thicknesses, it is evident that the cut-off scale decreases faster than the thickness, regardless of the definition of the latter. In order to assess a possible power-law scaling with pressure of the cut-off scale, Fig. 3(b) shows the same results in logarithmic scales. First of all,

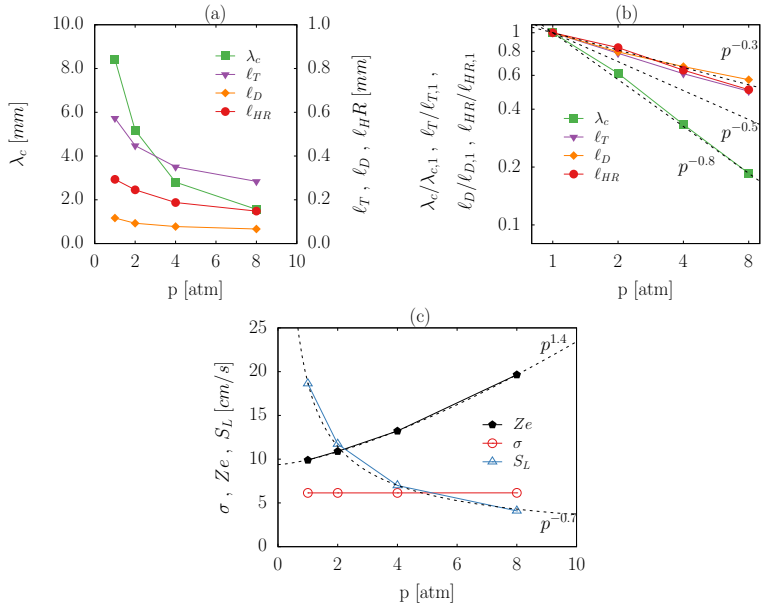

Figure 3: Comparison of the pressure dependence of the thermal (triangles), diffusive (diamonds), and reaction-layer (circle) flame thickness with the cut-off length scale of the hydrodynamics instability in linear (a) and logarithmic (b) scale. In (b) the results are normalized with the values at $p = 1$ atm; the dashed lines indicate different power-law pressure scaling. (c) Pressure dependence of the Zeldovich number (pentagons), expansion ratio σ (open circles), and laminar flame speed S_L (open triangles). All results are shown for the methane-air flame at $T_u = 300$ K, $\phi = 0.7$, unity Lewis numbers computed with the multi-step chemistry model

this plot reveals that all the flame thicknesses have similar power-law scaling with an exponent close to -0.3, in agreement with the work of Dahoe and De Goey [42]. In addition, it is observed that the cut-off length scale λ_c obeys a power-law scaling $\lambda_c \propto p^{-0.8}$, which is remarkably different from the scaling of the flame thicknesses. In conclusion, it is found that the non-dimensional cut-off scales with the power law $\lambda_c/\ell_T \propto \lambda_c/\ell_D \propto p^{-0.5}$, regardless of the definition of the flame thickness. Additional quantities characterizing the

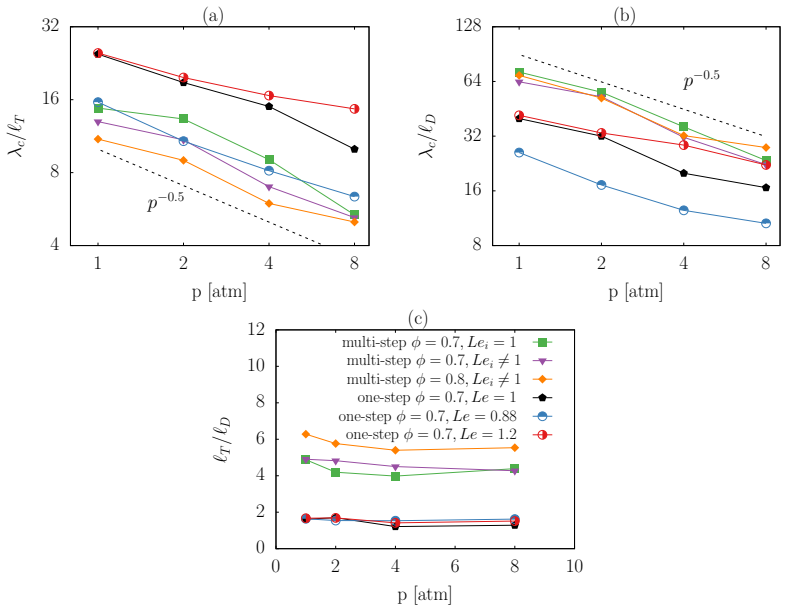

Figure 4: Dependency of the cut-off scale λ_c on pressure for: the multi-step chemistry with $T_u = 300$ K, $\phi = 0.7$, $Le_i = 1$ (green squares), $T_u = 300$ K, $\phi = 0.7$, $Le_i \neq 1$ (purple triangles), $T_u = 300$ K, $\phi = 0.8$, $Le_i \neq 1$ (orange diamonds), and for the one-step chemistry at with parameters corresponding to a methane air flame at $T_u = 300$ K, $\phi = 0.7$ and $Le = 1$ (black pentagons), $Le = 0.88$ (blue circles), $Le = 1.22$ (red circles). The results are scaled with the thermal (a) and diffusive thickness (b). The dashed lines indicate the scaling $p^{-0.5}$. (c) Ratio of the thermal and diffusive thicknesses for the same cases.

effect of pressure on the flame are shown in Fig. 3(c). As expected given the scaling of the thickness, the laminar flame speed scales with the power law $p^{-0.7}$ [42]. It is worth noting that the expansion ratio $\sigma = \rho_b/\rho_u$ has no dependence on pressure; this is expected since the temperature of the fresh mixture is kept constant when pressure is varied and the equilibrium temperature is virtually independent of pressure. The dependence of the Zeldovich number on pressure is well approximated by a scaling $p^{1.4}$. These

quantities are shown because they are the input parameters of the single-step chemistry model presented below.

The same analysis has also been applied for additional cases at different conditions shown in Fig. 4. Regardless of the conditions and the value of the Lewis numbers, the significant decrease of the normalized cut-off length scale is observed for higher pressure both normalizing with the thermal and the diffusive thickness.

Figure 4 shows also three cases computed with the one-step chemistry approach. The parameters Ze and σ in Eqs. 1 and 2 have been chosen to match those of the multi-step chemistry at $T_u = 300$ K and $\phi = 0.7$. For the $Le = 1$ case, the value selected for the 4 different pressures $\{1;\ 2;\ 4;\ 8\}$ atm are $Ze = \{9.89;\ 10.89;\ 14;\ 19.64\}$ (cf. Fig 4) and a constant expansion ratio $\sigma = 6.14$. The same values are used also for the one-step chemistry cases at $Le = 0.88$ and $Le = 1.22$. The one-step model can capture accurately the pressure scaling of the non-dimensional cut-off λ_c/ℓ_T and λ_c/ℓ_D already observed with the multi-step chemistry, while differences are observed in the actual values. The quantitative disagreement can be explained by the different flame models which yield a different, albeit similar, internal flame structure and a different ratio of thermal to diffusive thicknesses. In spite of the differences, these results clearly show that the pressure dependence of non-dimensional cut-off observed in the full multi-step DNS can be reproduced in the one-step approach if variations of the Zeldovich number are appropriately included. This fact also suggests that the main reason for the observed pressure dependence is a different profile of the reaction rate, which is mainly parametrized by the Zeldovich number. The Zeldovich number,

as also suggested by the expression $Ze = 4(T_b - T_u)/(T_b - T_0)$, is related to the value of the cross-over temperature T_0, since the unburned T_u and fully burned T_b temperature do not change appreciably with pressure. The increase of T_0 with pressure is related to the balance between chain branching and chain breaking reactions. T_0 is the temperature at which the chain branching reactions (mainly $H + O_2 \rightarrow OH + O$) are balanced by the chain breaking reactions (mainly $H + O_2 + M \rightarrow HO_2 + M$), which are often three-body reactions. For larger (smaller) temperature than T_0, the chain branching (chain breaking) reaction prevails. If pressure increases, chain breaking increases relative to chain branching due to the three-body reaction and the balance of the two occurs at higher temperature, increasing the Zeldovich number. Given the typical shape of the dispersion relations in Fig. 2, which shows that the wavelength of maximum growth λ_{max} is approximately twice the cut-off scale λ_c, λ_{max} is expected to scale with pressure in the same way of λ_{max}. While the present analysis is limited to methane combustion, the importance of radical recombination typically increases at higher pressure independently of fuel. The observed increase of Ze with pressure and the impact on λ_c should therefore hold for most fuels. In addition, since the single-step chemistry formulation would be the same the for different fuels, a similar behavior for the effect of Ze on λ_c is expected.

The DNS results can be summarized in the following way. Employing the multi-step chemistry, it is observed that the increase of pressure and the subsequent decrease of the cut-off lengthscale are associated with a significant increase of the Ze number and a negligible variation of the expansion ratio; for the methane combustion case considered here, the Lewis numbers do not

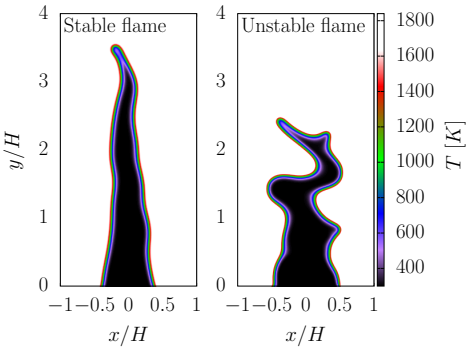

Figure 5: Visualization of the temperature field in the SP-1 stable and UP-8 unstable slot-burner flames.

play a role as well. Therefore, the dependence of λ_c on pressure is related to the dependence of Ze on pressure since the other non-dimensional parameters remain constant if pressure changes. Since the full set of equations for the multi-step model is difficult to analyze in its non-dimensional form and the different non-dimensional parameters cannot be specified independently, the non-dimensional system for the single-step chemistry has been also employed. A variation of only the Ze number, while the expansion ratio σ and the Lewis number are kept constant, causes a change of the non-dimensional cut-off length scale, in agreement with the observation in the multi-step simulations.

Finally, it is interesting to discuss the pressure dependence of the cut-off scale in the context of analytical models. It is worth noting that the theoretical analyses available in the literature [1, 13, 14] do not show an explicit dependence of the cut-off scale on pressure and its relation with the Zeldovich number. The dispersion relation derived from asymptotic analyses is typically written as [1]:

$$\omega(k) = \omega_0 S_L k - \ell_D [B_1 + Ze(Le-1)B_2 + PrB_3] S_L k^2 \qquad (3)$$

where the coefficients ω_0 and B_j are positive and depend only on the expansion ratio σ and Pr is the Prandtl number. Since the expansion ratio σ and the Prandtl number Pr are virtually independent of pressure, the pressure dependence of the value of k at which $\omega(k) = 0$ (the cut-off scale λ_c) could be ascribed to the term $Ze(Le - 1)B_2$ only when the Lewis number is not one. However, the pressure dependence of the cut-off scale has been observed also for unity Lewis number, as shown in Fig. 4; therefore, it is possible to conclude that Eq. 3 does not include the pressure effect observed in the DNS. The theoretical relation in Eq. 3 is truncated at the second order and, as noted by Matalon [1], should be extended with a forth (or even higher) order term to provide a comprehensive characterization of short wavelength stabilization. The coefficient of the forth order term, contrary to the second order one, was never derived explicitly in the context of hydrodynamic theory, with the exception of the scaling proposed by Sivashinsky [11] only valid for weak thermal expansion [1]. Therefore, it is reasonable to assume that the fourth order term may depend on all the non-dimensional parameters, including the expansion ratio and the Lewis and Zeldovich numbers. It follows that either the pressure dependence should be related to the fourth and higher order terms or that some of the hypotheses used to derive Eq. 3 should be relaxed and the coefficient of the second order term be modified to include a pressure dependence, possibly via a dependence on Ze that does not disappear for unity Lewis number.

3.2. Non linear regime: flame morphology at different pressures in a Bunsen burner

In order to observe flame instability in a Bunsen burner, the overall dimension of the flame surface needs to be large enough to accommodate unstable wavelengths, i.e., larger than the cut-off length scale λ_c. It has been shown extensively [18], that the jet slot width H can be appropriately used as a measure of the overall flame dimension. In this study, it was observed that characteristic signatures of the instability were present if the slot width H was larger than the cut-off scale λ_c. Therefore, we consider two Bunsen flames, at different pressures ($p = 1$ atm, SP-1 and $p = 8$ atm UP-8), with the same slot width H, measured in units of flame thickness ℓ_T, $H = 12\ell_T$, c.f. Tab. 1. Knowing that the normalized cut-off scale λ_c/ℓ_T is significantly different at the two different pressures, the two cases at $p = 1$ atm and $p = 8$ atm are characterized by a slot width smaller and larger than the cut-off scale, respectively. Figure 5 shows a visualization of the temperature field for $p = 1$ atm (SP-1) and $p = 8$ atm (UP-8). It is evident that the flame at higher pressure features a significantly higher flame wrinkling and the presence of typical Darrieus-Landau cusps with high negative curvature. It is worth noting that, for the low-pressure case, the only significant cusp is at the flame tips and is not ascribed to intrinsic instability. The flame morphology is statistically analyzed in terms of the probability density functions PDF of the flame front curvature as shown in Fig. 6. The PDF of the UP-8 case is wider than that of the SP-1 case with a more pronounced negative tail. The large negative values of curvature in the SP-1 case are, as noted above, related to the flame tip. The skewness of the two distributions, which has

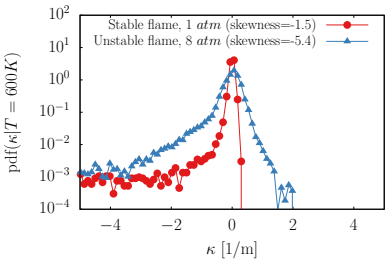

Figure 6: Probability density function of the flame front curvature, conditioned at $T = 600K$, for the SP-1 stable flame (red circles) and UP-8 unstable flame (blue triangles).

been recently used as a marker of Darrieus-Landau instability [18, 21, 25], is -1.5 and -5.4 for the case at $p = 1$ atm (SP-1) and at $p = 8$ atm (UP-8), respectively, confirming the presence of instability only in the high pressure flame. These observations confirm that the effect of pressure in the non-linear regime is akin to that observed in the linear phase.

4. Conclusions

The effect of pressure on the hydrodynamic stability limits of methane-air flames has been studied with DNS. It is found that the cut-off length scale λ_c between stable and unstable perturbations decreases significantly with pressure and that this behavior cannot be ascribed completely to the decrease of flame thickness, since the pressure scaling of the cut-off $\lambda_c \approx p^{-0.8}$ is significantly steeper than the pressure scaling of both the thermal $\ell_T \approx p^{-0.3}$ and diffusive thickness $\ell_D \approx p^{-0.3}$. This behavior is observed also with a one-step chemistry approach if the Zeldovich number appearing in the model is varied according to the results from multi-step chemistry to take into account variations of the cross-over temperature, which are caused by increasing importance of chain-breaking reactions at high pressure. Finally,

the strong variation with pressure of the normalized cut-off λ_c/ℓ_T has been observed also in two-dimensional slot flames characterized, when unstable, by the cusp-like structures typical of the non-linear regime of the hydrodynamics instability.

Acknowledgements

The authors acknowledge funding from of the European Research Council (ERC) under the European Unions Horizon 2020 research and innovation program under grant agreement No 695747.

References

[1] M. Matalon, Intrinsic flame instabilities in premixed and nonpremixed combustion, Annu. Rev. Fluid Mech. 39 (2007) 163–191.

[2] G. Darrieus, Propagation d'un front de flamme, La Technique Moderne 30 (1938) 18.

[3] L. D. Landau, On the theory of slow combustion, Acta Physicochimca (USSR) 19 (1944) 77–85.

[4] H. Kobayashi, H. Kawazoe, Flame instability effects on the smallest wrinkling scale and burning velocity of high-pressure turbulent premixed flames, Proc. Combust. Inst. 28 (2000) 375–382.

[5] H. Kobayashi, Y. Kawabata, K. Maruta, Experimental study on general correlation of turbulent burning velocity at high pressure, Symp. (Int.) Combust. 27 (1998) 941–948.

[6] G. Troiani, F. Creta, M. Matalon, Experimental investigation of Darrieus–Landau instability effects on turbulent premixed flames, Proc. Combust. Inst. 35 (2015) 1451–1459.

[7] V. R. Savarianandam, C. J. Lawn, Burning velocity of premixed turbulent flames in the weakly wrinkled regime, Combust. Flame 146 (2006) 1–18.

[8] S. Yang, A. Saha, Z. Liu, C. K. Law, Role of Darrieus–Landau instability in propagation of expanding turbulent flames, J. Fluid Mech. 850 (2018) 784–802.

[9] C. Clanet, G. Searby, First experimental study of the Darrieus-Landau instability, Phys. Rev. Lett. 80 (1998) 3867.

[10] J. Beeckmann, R. Hesse, S. Kruse, A. Berens, N. Peters, H. Pitsch, M. Matalon, Propagation speed and stability of spherically expanding hydrogen/air flames: Experimental study and asymptotics, Proc. Combust. Inst. 36 (2017) 1531–1538.

[11] G. I. Sivashinsky, Nonlinear analysis of hydrodynamic instability in laminar flames—I. Derivation of basic equations, Acta astronautica 4 (1977) 1177–1206.

[12] G. I. Sivashinsky, P. Clavin, On the nonlinear theory of hydrodynamic instability in flames, Journal de Physique 48 (1987) 193–198.

[13] V. Akkerman, V. Bychkov, Turbulent flame and the Darrieus-Landau instability in a three-dimensional flow, Combust. Theor. Model. 7 (2003) 767–794.

[14] V. Akkerman, V. Bychkov, Velocity of weakly turbulent flames of finite thickness, Combust. Theor. Model. 9 (2005) 323–351.

[15] M. Matalon, F. Creta, The turbulent flame speed of wrinkled premixed flames, Comptes Rendus Mécanique 340 (2012) 845–858.

[16] Y. Rastigejev, M. Matalon, Nonlinear evolution of hydrodynamically unstable premixed flames, J. Fluid Mech. 554 (2006) 371–392.

[17] F. Creta, N. Fogla, M. Matalon, Turbulent propagation of premixed flames in the presence of Darrieus–Landau instability, Combust. Theor. Model. 15 (2011) 267–298.

[18] F. Creta, R. Lamioni, P. E. Lapenna, G. Troiani, Interplay of Darrieus-Landau instability and weak turbulence in premixed flame propagation, Phys. Rev. E 94 (2016) 053102.

[19] L. Berger, K. Kleinheinz, A. Attili, H. Pitsch, Characteristic patterns of thermodiffusively unstable premixed lean hydrogen flames, Proc. Combust. Inst. 37 (2019) 1879–1886.

[20] R. Yu, X.-S. Bai, V. Bychkov, Fractal flame structure due to the hydrodynamic Darrieus-Landau instability, Phys. Rev. E 92 (2015) 063028.

[21] R. Lamioni, P. E. Lapenna, G. Troiani, F. Creta, Flame induced flow features in the presence of Darrieus-Landau instability, Flow Turb. Comb. 101 (2018) 1137–1155.

[22] R. Lamioni, P. E. Lapenna, G. Troiani, F. Creta, Strain rates, flow pat-

terns and flame surface densities in hydrodynamically unstable, weakly turbulent premixed flames, Proc. Combust. Inst. 37 (2019) 1815–1822.

[23] P. E. Lapenna, R. Lamioni, G. Troiani, F. Creta, Large scale effects in weakly turbulent premixed flames, Proc. Combust. Inst. 37 (2019) 1945–1952.

[24] F. Creta, P. E. Lapenna, R. Lamioni, N. Fogla, M. Matalon, Propagation of premixed flames in the presence of Darrieus–Landau and thermal diffusive instabilities, Combust. Flame 216 (2020) 256–270.

[25] M. Klein, H. Nachtigal, M. Hansinger, M. Pfitzner, N. Chakraborty, Flame Curvature Distribution in High Pressure Turbulent Bunsen Premixed Flames, Flow Turb. Comb. 101 (2018) 1173–1187.

[26] T. Poinsot, D. Veynante, Theoretical and numerical combustion, RT Edwards, Inc., 2005.

[27] A. Attili, F. Bisetti, M. E. Mueller, H. Pitsch, Formation, growth, and transport of soot in a three-dimensional turbulent non-premixed jet flame, Combust. Flame 161 (2014) 1849–1865.

[28] S. Luca, A. Attili, E. Lo Schiavo, F. Creta, F. Bisetti, On the statistics of flame stretch in turbulent premixed jet flames in the thin reaction zone regime at varying Reynolds number, Proc. Combust. Inst. 37 (2019) 2451–2459.

[29] A. Attili, S. Luca, D. Denker, F. Bisetti, H. Pitsch, Turbulent flame speed and reaction layer thickening in premixed jet flames at

constant Karlovitz and increasing Reynolds numbers, arXiv preprint arXiv:2005.04040 (2020).

[30] S. Luca, A. N. Al-Khateeb, A. Attili, F. Bisetti, Comprehensive Validation of Skeletal Mechanism for Turbulent Premixed Methane–Air Flame Simulations, J. Propul. Power 34 (2017) 153–160.

[31] A. Attili, F. Bisetti, M. E. Mueller, H. Pitsch, Effects of non-unity Lewis number of gas-phase species in turbulent nonpremixed sooting flames, Combust. Flame 166 (2016) 192–202.

[32] O. Desjardins, G. Blanquart, G. Balarac, H. Pitsch, High order conservative finite difference scheme for variable density low Mach number turbulent flows, J. Comput. Phys. 227 (2008) 7125–7159.

[33] X. Liu, S. Osher, T. Chan, Weighted essentially non-oscillatory schemes, J. Comput. Phys. 115 (1994) 200–212.

[34] A. Hindmarsh, P. Brown, K. Grant, S. Lee, R. Serban, D. Shumaker, C. Woodward, SUNDIALS: Suite of nonlinear and differential/algebraic equation solvers, ACM Transactions on Mathematical Software (TOMS) 31 (2005) 363–396.

[35] H. Pitsch, FlameMaster, a C++ computer program for 0D combustion and 1D laminar flame calculations, Technical Report, University of Technology (RWTH) Aachen, 1998.

[36] N. Peters, F. A. Williams, The asymptotic structure of stoichiometric methane air flames, Combust. Flame 68 (1987) 185–207.

[37] C. K. Law, Combustion Physics, Cambridge University Press, 2010.

[38] P. E. Lapenna, F. Creta, Mixing under transcritical conditions: An a-priori study using direct numerical simulation, J. Sup. Fluids 128 (2017) 263–278.

[39] P. E. Lapenna, Characterization of pseudo-boiling in a transcritical nitrogen jet, Phys. Fluids 30 (2018) 077106.

[40] P. E. Lapenna, F. Creta, Direct Numerical Simulation of Transcritical Jets at Moderate Reynolds Number, AIAA J. 57 (2019) 2254–2263.

[41] A. T. Patera, A spectral element method for fluid dynamics: laminar flow in a channel expansion, J. Comput. Phys. 54 (1984) 468–488.

[42] A. E. Dahoe, L. P. H. De Goey, On the determination of the laminar burning velocity from closed vessel gas explosions, Journal of Loss Prevention in the Process Industries 16 (2003) 457–478.